Acta Crystallographica Section A
Foundations of Crystallography
ISSN 0108-7673

Received 28 May 2007
Accepted 8 August 2007

Can the interaction density be measured? The example of the non-standard amino acid sarcosine

B. Dittrich* and M. A. Spackman

Chemistry, M313, School of Biomedical, Biomolecular and Chemical Sciences, University of Western Australia, Crawley, WA 6009, Australia. Correspondence e-mail: birger@cyllene.uwa.edu.au

The experimental charge density $\rho(\mathbf{r})$ of the non-standard amino acid sarcosine has been determined based on an extensive and complete data set measured at 100 K to high resolution ($\sin\theta/\lambda = 1.18$ Å^{-1}) by single-crystal X-ray diffraction. Anisotropic thermal motion of the H atoms, obtained from TLS + ONIOM cluster methods, was included in the structural model. Based on the multipole-model geometry, the theoretical Hartree–Fock interaction density of a molecule in the crystal has been calculated with *CRYSTAL98*. It manifests itself in local rearrangements of $\rho(\mathbf{r})$ and can be reproduced with a multipole projection *via* simulated structure factors. An attempt has also been made to obtain the interaction density from a combination of experimental and theoretical charge densities using either a whole-molecular calculation or the invariom database. Agreement with the periodic Hartree–Fock interaction density is qualitative. It is shown that invarioms reproduce the features of the theoretical multipole-projected whole-molecular electron density, and can be used to approximate it.

1. Introduction

The interaction density is the difference between an electron distribution for the crystal and a superposition of non-interacting molecules. A high-resolution X-ray diffraction experiment followed by a multipole refinement reveals the electron density of the crystal, hence it may be used to obtain the interaction density. To study this effect *ab initio* is computationally demanding and time consuming since periodic calculations are required. Obtaining the interaction density theoretically is therefore limited by the size of the system, the level of approximation and the basis set used. Pioneering crystal Hartree–Fock studies on urea (Gatti *et al.*, 1994), ice VIII (Gatti *et al.*, 1995) and HCN (Platts & Howard, 1996) have nevertheless analyzed the effects of intermolecular interactions by focusing directly on the electron distribution from the wavefunction.

A detailed theoretical study of the effect of intermolecular interactions has been performed by Spackman *et al.* (1999), who projected electron densities onto a multipole model by refining against simulated structure factors for ice VIII, acetylene, formamide and urea. That study concluded that the multipole model is capable of qualitative retrieval of the interaction density, despite known shortcomings in the model itself. Although the study of Spackman *et al.* included the effects of thermal motion on the refined electron densities, no account was taken of the effect of random errors (noise) in the simulated structure factors. According to de Vries *et al.* (2000), addition of noise to theoretical observations for urea made it impossible to retrieve the interaction density for simulated data.

Our interest in the interaction density is fueled by the aim to improve the prediction of the electron-density distribution in the crystal beyond the superposition of isolated molecules for invariom modeling. Although there is no direct physical significance of the interaction density, its understanding will improve the prediction of molecular properties in the bulk from isolated molecular densities. As a difference density, the interaction density also shows the response of the molecular electron density to an external perturbation, here the surrounding molecules in the crystal.

The main aim of this paper is to demonstrate that qualitative features of the interaction density can in principle be obtained from a combination of theory and experiment, even for a non-centrosymmetric structure. Here we have determined the experimental charge density of the non-standard amino acid sarcosine to study the interaction density in detail for a small system that can be conveniently handled by a full quantum-mechanical treatment. Experimental data reach a high quality as indicated by low internal R factors and an $R_w(F)$ of 1%. A periodic Hartree–Fock result serves as a benchmark to a multipole projection and we initially investigate the effect of the density representation.

Additionally, we propose new methodology to obtain an approximate 'experimental' interaction density for larger molecules based on a 'whole molecular' or the invariom approach (Dittrich *et al.*, 2004), combining theory and experiment. The first step involved is the acquisition of

single-crystal X-ay diffraction data extending to high scattering angles. These data are fitted in reciprocal space by least-squares methods with the pseudoatom formalism (Stewart, 1976<bbr id=), here in the form of the Hansen & Coppens (1978) multipole model. The atomic positions and anisotropic displacement parameters (ADPs) of the non-H atoms are obtained by invariom scattering factors. Subsequently, an experimental multipole refinement based on the same multipole model provides the electron density in the crystal. Ultimately, our aim was to obtain the interaction density as the difference between experimental and theoretical (or invariom database) densities using the same geometry. To verify that the fragment-based invariom density is similar to the isolated molecular theoretical density, we have also computed the difference between a 'whole molecule' single-point electron density fitted with multipoles and the invariom density. In order to observe fine features of the electron-density distribution like the interaction density, it is necessary to include an accurate description of the thermal motion of the H atoms (Madsen *et al.*, 2004) and we will describe how their ADPs were derived from a QM/MM cluster calculation (Whitten & Spackman, 2006).

The interaction density, being a simple difference, is conceptually very easy to understand. Unfortunately, practical difficulties arise: on one hand, we do not know exactly how well the full periodic theoretical treatment agrees with the experimental density. On the other hand, the isolated-molecular density that we subtract can be calculated with different basis sets or generated from a database. Finally, the density representation between experiment and theory differs, so that we have to project the theoretical density onto the multipole model for comparison. We hope that the reader will not forget that the broader scope is to obtain a conceptually simple difference density.

Table 1
Crystal and structure refinement data for sarcosine.

Empirical formula	$C_3H_7NO_2$	
Formula weight (g mol^{-1})	89.10	
Cell setting, space group	Orthorhombic, $P2_12_12_1$ (No. 19)	
Z	4	
Temperature (K)	100 (1)	
Unit-cell dimensions		
a (Å)	6.6558 (1)	
b (Å)	7.8903 (1)	
c (Å)	8.6069 (1)	
V (Å^3)	452.01 (2)	
Calculated density (g cm^{-3})	1.3093	
$F(000)$	192.0	
Crystal size (mm)	0.32 × 0.39 × 0.48	
Crystal form, color	Tetrahedron, colorless	
Wavelength λ (Å)	0.7107	
Absorption coefficient μ (mm^{-1})	0.11	
Absorption correction	Face indexed analytical	
T_{min}/T_{max}	0.969/0.977	
Max. θ (°)	57.19	
$(\sin\theta/\lambda)_{max}$ (Å^{-1})	1.18	
Measured, independent and observed reflections	78770, 3555, 2927	
Criterion for observed reflections	$F > 2.5\sigma(F)$	
Overall completeness	99.8%	
Redundancy	22.1	
Weighting scheme	Based on measured s.u.'s†	
$R_{int}(F^2)$‡	0.027	
	EXPER_INVM	*EXPER_MULT*
Number of parameters	83	83 + 73§
N_{ref}/N_{var}	35.27	26.85
$R_1(F)$‡	1.72	1.66
$R_w(F)$‡	1.15	1.04
$R_{all}(F)$	2.47	2.41
S‡	1.89	1.71
$\Delta\rho_{max}$, $\Delta\rho_{min}$(e Å^{-3})	0.20, −0.14	0.17, −0.16

† $w = 1/\sigma^2$. ‡ $R_{int}(F^2) = \sum|F_o^2 - F_o^2(\text{mean})|/\sum F_o^2$, $R_w(F) = \sum w||F_o| - k|F_c||/\sum w|F_o|$, $R_1(F) = \sum||F_o| - k|F_c||/\sum|F_o|$, $R_{all}(F)$ includes all reflections, $S = [\sum w||F_o| - k|F_c||^2)/(n_o - m_{var})]^{1/2}$. § Some parameters, *e.g.* κ's, were fixed at invariom values, see text.

2. Experimental

A single crystal of the title compound was selected from the commercially obtained (Sigma Aldrich) sample. A single-crystal X-ray diffraction experiment was carried out at 100 K on an Oxford Diffraction Xcalibur S diffractometer equipped with a nitrogen gas-stream cooling device. *CrysAlis RED* (Oxford Diffraction Ltd, 2006) was used for data reduction and for the face-indexed analytical absorption correction (Clark & Reid, 1995). Excellent crystal quality and scattering power allowed measurement of data to a resolution of $\sin\theta/\lambda_{max} = 1.18$ Å^{-1} with an overall coverage of 99.8% and an internal R factor of 2.8% within 3 d. No significant intensity decay was observed and the detector-to-crystal distance was 42 mm; every frame covered 1° in ω or ϕ.

The measurement strategy and further crystallographic details can be found in Table 1.[1] The atomic numbering scheme is depicted in an *ORTEP* (Burnett & Johnson, 1996) representation of the structure in Fig. 1.

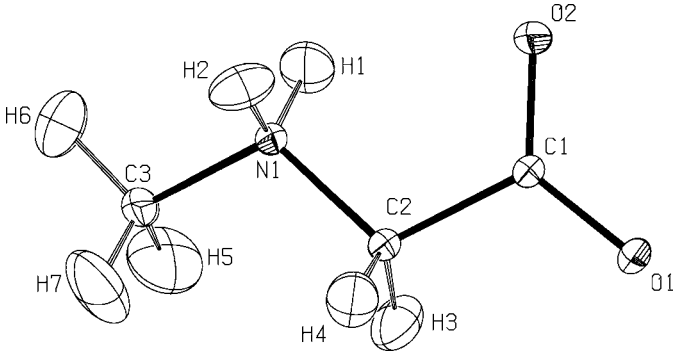

Figure 1
ORTEP representation (Burnett & Johnson, 1996) of the experimentally determined molecular structure in the crystal with atomic numbering scheme and thermal ellipsoids with 50% probability.

[1] Supplementary data for this paper are available from the IUCr electronic archives (Reference: SH5061). Services for accessing these data are described at the back of the journal.

3. Calculation of anisotropic thermal motion of H atoms

For this investigation, H-atom ADPs are especially relevant, as they can influence not only the X—H bond topology and character, but also the electron density of neighboring atoms (Madsen *et al.*, 2004). Obtaining H-atom ADPs is therefore an important area of current charge-density research (Roversi & Destro, 2004; Dittrich *et al.*, 2005; Madsen, 2006). ADPs for H atoms were calculated using the recently introduced TLS + ONIOM method (Whitten & Spackman, 2006). A C computer program was written to build molecular clusters and write *Gaussian* input files (Dittrich, 2007) for this QM/MM method (Dapprich *et al.*, 1999). The chosen cluster consisted of 15 sarcosine molecules with 195 atoms in total (Fig. 2). Only the central molecule was included in the high layer of the ONIOM calculation [basis set HF/6-31G(d,p)], while all other molecules were part of the low layer [UFF force field (Rappé *et al.*, 1992)].

Potential-derived atomic point charges were included in the calculation, obtained from a single-point energy calculation (Besler *et al.*, 1990) at the invariom geometry. The converged geometry optimization in the cluster provided 'internal' frequencies and normal modes that were transformed into ADPs in the Cartesian crystal system with the *XDVIB1/2* programs of the *XD* package (Koritsánszky *et al.*, 2003), omitting the lowest six normal modes. In the TLS + ONIOM approach, these 'internal' contributions to the ADPs are subtracted from the experimental ADPs from a high-angle spherical-atom refinement of the non-H atoms and the remaining contributions subsequently subjected to a **TLS** fit with the program *THMA11* (Schomaker & Trueblood, 1968, 1998). The outcome, the rigid-body contribution to ADPs uncontaminated by the 'internal' modes, was then added to the calculated contributions from the internal modes for the H atoms. The *ORTEP* (Burnett & Johnson, 1996) plot in Fig. 1 includes the H-atom ADPs derived in this way.

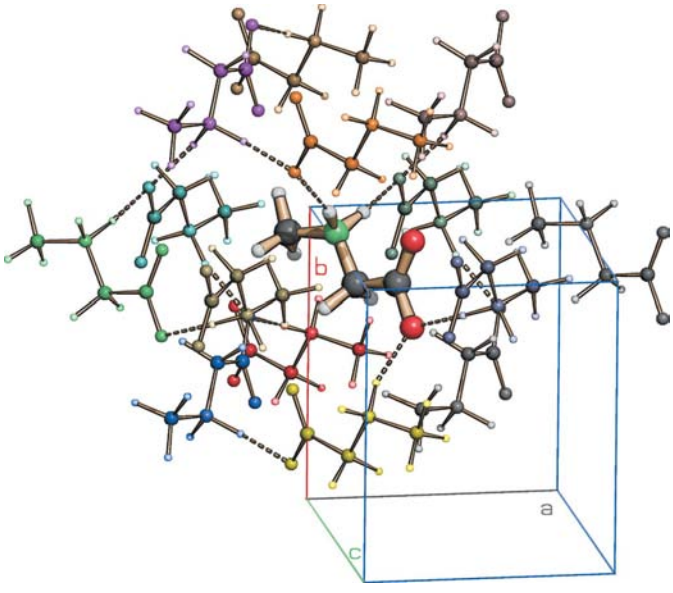

Figure 2
SCHAKAL99 (Keller & Pierrard, 1999) representation of the cluster used in the ONIOM calculation, emphasizing the central molecule and including hydrogen bonding.

4. Charge density and invariom refinement

Data were refined and modeled using the Hansen & Coppens multipole formalism (Hansen & Coppens, 1978; Coppens, 1997) as implemented in the least-squares program *XDLSM* of the program package *XD* (Koritsánszky *et al.*, 2003). The multipole formalism describes the static electron density $\rho(\mathbf{r})$ by atom-centered multipole functions. To obtain the model electron densities for a fit of experimental or simulated structure factors, multipole parameters κ, κ', P_v and P_{lm} [equation (1)] were refined by reciprocal-space least-squares refinements.

$$\rho_{\rm atom}(\mathbf{r}) = \rho_{\rm core}(r) + P_v\kappa^3\rho_v(\kappa\mathbf{r}) + \sum_{l=0}^{l_{\rm max}} \kappa'^3 R_l(\kappa'\mathbf{r}) \sum_{m=0}^{l} P_{lm\pm} d_{lm\pm}(\theta,\phi). \quad (1)$$

Core and spherical valence density (ρ_v) of the heavy atoms are obtained from Hartree–Fock wavefunctions expanded over Slater-type basis functions (Clementi & Raimondi, 1963). For the deformation terms, single-ζ orbitals with energy-optimized Slater exponents are employed and kept fixed (Clementi & Roetti, 1974). The parameters of the radial functions are obtained by weighting single-ζ orbitals by their occupation, and exponents are κ-adjusted modifying standard molecular values (Hehre *et al.*, 1969, 1970). Based on the structure of sarcosine originally determined (Mostad & Natarajan, 1989), the refinement was initiated with *SHELXL* (Sheldrick, 1997), thereby providing starting atomic parameters for subsequent invariom and multipole refinements. In the following refinements, the quantity $\sum_{\mathbf{H}} w_{\mathbf{H}}[|F_{\rm obs}(\mathbf{H})| - k|F_{\rm cal}(\mathbf{H})|]^2$ was minimized using the statistical weight $w_{\mathbf{H}} = \sigma^{-2}(F_{\rm obs}(\mathbf{H}))$.

4.1. Invariom refinement

In the next step, an invariom refinement was carried out (*EXPER_INVM*). Input files for subsequent refinements were prepared with the *INVARIOMTOOL* program (Hübschle *et al.*, 2007). Electroneutrality of the asymmetric unit was achieved by scaling of database monopole populations based on Allred–Rochow electronegativity (EN) (Allred & Rochow, 1958) of the elements in the structure. The difference between the sum of the monopole populations from the database and neutral atoms was 0.14% of the total valence charge of 36 e in the asymmetric unit, corresponding to a correction of 0.05 e. Invariom scattering factors, local atomic site symmetry and the model compounds used can be found in Table 2; full details of the modeling procedure were recently reported (Hübschle *et al.*, 2007). For the refinement of model compounds, the order of the multipole expansion included hexadecapoles for all atoms (P_v and P_{lm}). Parameters to refine taking into account local atomic site symmetry were chosen according to the rules given by Kurki-Suonio (1977). Refined H-atom positions gave

Table 2
Details of invariom and experimental refinement on sarcosine.

Atom label	Invariom assigned (*EXPER_INVM*)	Site symmetry (*EXPER_INVM* & *_MULT*)	Model compound (*EXPER_INVM*)	Chemical constraints (*EXPER_MULT*)
O(1)	O1.5c[1.5o1c]$^-$	*m*	Formic acid anion	
O(2)	O1.5c[1.5o1c]$^-$	*m*	Formic acid anion	O(1)
N(1)	N1c1c1h1h$^-$	*mm*2	Dimethylamine cation	
C(1)	C1.5o1.5o1c$^-$	*m*	Formic acid anion	
C(2)	C1n1c1h1h$^+$	1	Aminoethane cation	
C(3)	C1n1h1h1h$^+$	3	Aminomethane cation	
H(1)	H1n[1c1c1h]$^+$	6	Dimethylamine cation	
H(2)	H1n[1c1c1h]$^+$	6	Dimethylamine cation	H(1)
H(3)	H1c[1n1c1h]	6	Aminoethane	
H(4)	H1c[1n1c1h]	6	Aminoethane	H(3)
H(5)	H1c[1n1h1h]$^+$	6	Aminomethane cation	
H(6), H(7)	H1c[1n1h1h]$^+$	6	Aminomethane cation	H(5)

bond distances to corresponding heavy atoms in good agreement with tabulated average neutron distances.

One advantage of the invariom procedure is that every scattering factor assigned to an atom in a structure can be identified by its name, which conveys meaning as it is directly related to the atom's chemical environment. By choosing model compounds that include a larger shell of the chemical environment of an atom of interest, any accuracy can be achieved in reproducing the theoretical density. Table 2 lists the scattering factors assigned. Automatically identified scattering factors C1n1h1h1h and C1n1c1h1h (Hübschle *et al.*, 2007) were replaced by C1n1h1h1h$^+$ and C1n1c1h1h$^+$, as this yields a slightly better reproduction of the isolated molecular density as explained in §5. This basically amounts to inclusion of next-nearest neighbors for atoms that are adjacent to a charged group like $-NH_3^+$.

4.2. Experimental multipole refinement

The multipole refinement *EXPER_MULT* was initiated with the result of the invariom refinement. Local atomic site symmetry and coordinate systems were chosen to be identical, and atomic positions, expansion/contraction parameters κ and ADPs were kept fixed at the *EXPER_INVM* results. Furthermore, multipole populations of H atoms were also kept fixed; only the multipole populations of the non-H atoms were adjusted against the experimental data. The total charge of the asymmetric unit was kept constant. To enable comparison with invariom modeling, chemical similarity, as defined by the invariom assigned, was mimicked by using chemical constraints for the respective atoms, as listed in Table 2. Agreement factors of the least-squares fit for *EXPER_INVM* and *EXPER_MULT* refinements can be found in Table 1. The deformation density map for the *EXPER_MULT* refinement shows typical features (see Fig. 6 below) and is in excellent agreement with the predicted invariom map.[2] No significant electron density was found in the residual density maps calculated including all reflections with $F > 2.5\sigma(F)$ (see below in Fig. 8). The Hirshfeld test (Hirshfeld, 1976) yielded a highest difference in mean-square displacement amplitudes (DMSDA) of 0.0007 Å^2, indicating satisfactory deconvolution of thermal motion and electron density.

[2] See deposition footnote.

5. Calculation of simulated structure factors

Simulated structure factors were obtained from two different programs. Those for a molecule in the crystal environment using the geometry from the *EXPER_INVM* refinement were obtained from the *PROPERTIES* routine of the *CRYSTAL98* package (Saunders *et al.*, 1998) using the *XFAC* keyword and the basis set 6-31G(d,p). The multipole model, described in the previous section, was then fitted to these simulated structure factors for the crystal environment (*THEOR_CRYS* refinement) to see how well the multipole model can recover information on the crystal-field effect.

Phases were replaced with theoretical ones (Koritsanszky *et al.*, 2002) at each refinement cycle with a locally modified version of *XDLSM*. This procedure was repeated with the density matrix obtained for a superposition of isolated molecules as obtained with *CRYSTAL98* using the *MOLSPLIT* option (*THEOR_SPLT*), which allowed us to obtain an interaction density within the density description of the multipole model.

As periodic Hartree–Fock (PHF) calculations have natural limitations concerning the size of the molecule investigated, we have also tried to obtain the electron density of a theoretically derived isolated molecule with the program *Gaussian98* (2002). A single-point B3LYP calculation with the standard basis set D95++(3df,3pd) was carried out based on the geometry from *EXPER_INVM* refinement. This basis set was chosen to allow a comparison between database density and the whole molecular result in §6.7. Again, simulated structure factors were calculated from the molecular wavefunction and were projected onto multipole parameters. From this isolated-molecule density, translated and placed in a cubic cell with lattice constants of 30 Å using space group *P*1,

complex theoretical structure factors were calculated. The Fourier transform of the Gaussian orbital products was derived analytically (Jayatilaka, 1994) with the program *TONTO* (Jayatilaka & Grimwood, 2003). The multipole model described in the previous section was then fitted to these theoretical structure factors (*THEOR_MOLE* refinement). Only multipoles and a scale factor were refined while positional parameters were kept fixed and the description of thermal movement was omitted, leading to an $R_1(F)$ of 0.4%. As for the *THEOR_CRYS* refinement, phases were replaced with theoretical ones at each refinement cycle. A resolution limit ($\sin\theta/\lambda = 1.15$ Å^{-1}) comparable to that of the experiment was used in this projection of the theoretical density onto multipole populations of the aspherical-atom formalism, and unit weights were applied. The multipole parameters obtained in this way served as a benchmark for the invariom database parameters in a comparison to the 'whole-molecule' electron density both represented by pseudoatomic fragments and allow the interaction density to be determined from experiment.

6. Results and discussion

6.1. Review of earlier studies

In their model study on the interaction density, Spackman *et al.* (1999) came to several conclusions that are highly relevant to this work.

(i) The effect of the interaction density peaks near a resolution of 0.2 Å^{-1} in reciprocal space and then decays monotonically. This behavior is different for the residual electron density, enabling one to distinguish between unmodeled features and the effect of intermolecular interactions.

(ii) The lack of sophistication of a particular model used does not compromise the principal ability of the multipole model to retrieve crystal-field effects on the electron distribution.

(iii) In the hydrogen-bonded systems formamide and urea, there was a flow of electron density from the donor to the acceptor of the order of magnitude of ≈0.1 e when identical multipole models were used. As the magnitude of the atomic charges (monopole populations) depends more on the sophistication of the multipole model than on the interaction density, the effect is hard to observe in the monopole populations.

(iv) *R*-factor differences between model structure factors for the bulk and the isolated molecule are likely to be rather small.

6.2. Differences in the figures of merit

The last point raised is supported by listings of the *R* factor for the *EXPER_MULT* and the *EXPER_INVM* refinements in Table 1. Local redistributions of density due to the interaction of molecules in the crystal explains why the invariom model *R* factor is 0.1% higher than the *EXPER_MULT* result. Improvements achieved with the constrained multipole refinement described above invoking more than twice as many parameters are small in terms of the *R* factor.

6.3. Calculation of the interaction density in the crystal

Based on purely theoretical methodology, for sarcosine we can come to very similar conclusions to those for urea and formamide (Gatti *et al.*, 1994; Spackman *et al.*, 1999).

The heavy-atom skeleton of sarcosine is almost planar, facilitating the visualization of the deformation of electron density in covalent bonds (Fig. 3*a*) or the redistribution due to intermolecular interactions. As can be seen in Fig. 3(*b*), most pronounced differences between crystal and molecular densities can be found near the O1 and O2 atoms, on the C1—C2 bond and on the C2—N1 bond. It appears that all these differences point towards N1, although they are due to hydrogen bonding to neighboring molecules. Quantitatively, one can observe that the highest features in the interaction

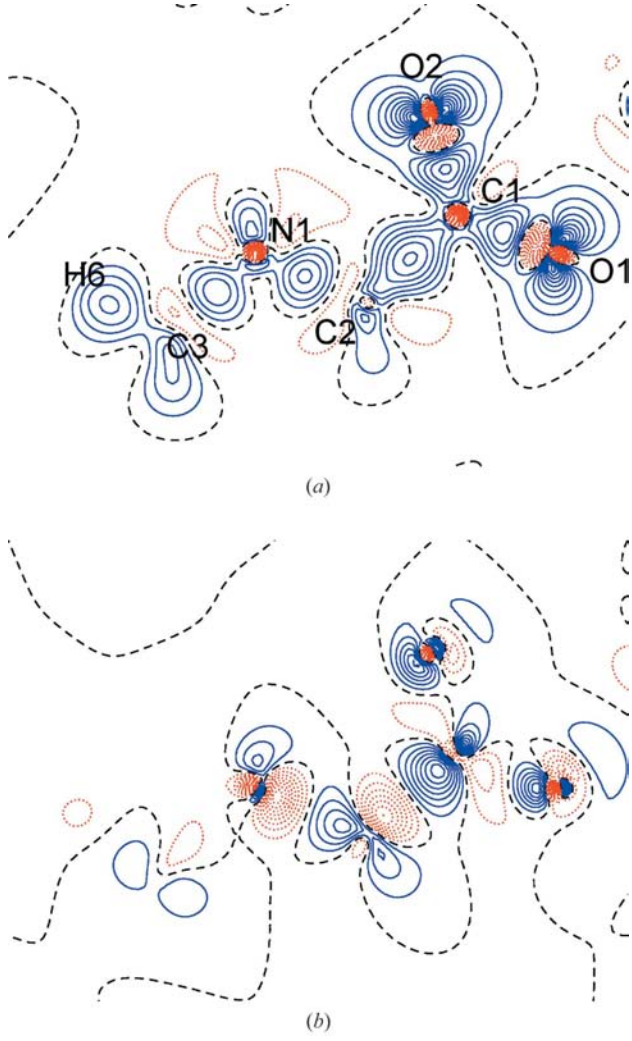

Figure 3
(*a*) Theoretical deformation density and (*b*) interaction density calculated from *CRYSTAL98* (Saunders *et al.*, 1998). For the deformation density (*a*) contour lines are 0.1 e Å^{-3}, while they are 0.025 e Å^{-3} in the interaction density (*b*) with blue indicating positive and red negative features.

density slightly exceed ≈0.15 e Å^{-3}, again agreeing with the trends observed earlier (Spackman *et al.*, 1999). One can conclude that the interaction density is a small but systematic effect, especially in relation to bonding density features that are *ca* five times stronger for typical covalent bonds and are shown for comparison on a different scale in Fig. 3(*a*). Whether the Hartree–Fock interaction density as calculated with the rather limited basis set 6-31G(d,p) displayed here really is close to the experimental electron density is not investigated here. It can be assumed that effects of intramolecular electron correlation not taken into account by the Hartree–Fock method play only a minor role (Bytheway *et al.*, 2007).

6.4. Projection onto the multipole model

The *CRYSTAL98* theoretical interaction density (Fig. 3*b*) contains very sharp features near the nuclei. It has been pointed out that there is an effect of including κ' parameters on the modeling of the density (Spackman & Byrom, 1996). In Fig. 4, we have fitted the same multipole model as used in the *EXPER_MULT* refinement to simulated structure factors for the crystal, *i.e.* the *THEOR_CRYS* refinement. When κ' parameters are included in the model (Fig. 4*b*), the Fourier residual map obtained is improved and unmodeled features near the O atoms are reduced. Both refinements included calculated phases of the *CRYSTAL98* calculation as described above. A similar result with respect to unmodeled features near the O atoms was obtained earlier (Spackman & Byrom, 1996) for formamide. κ' parameters are usually not accessible from experiment in a reliable way due to thermal motion and data resolution. It is well known that, even with simulated data to experimental resolution, individual κ' parameters for each of the higher multipoles cannot be refined (Volkov & Coppens, 2001). Use of a single κ' parameter for all higher multipoles allows convergence to be achieved with the *KEEP KAPPA* option in *XDLSM*. The value of κ' for the carboxylate O atoms for the bulk (1.46) is similar to the isolated-molecule result of 1.44.

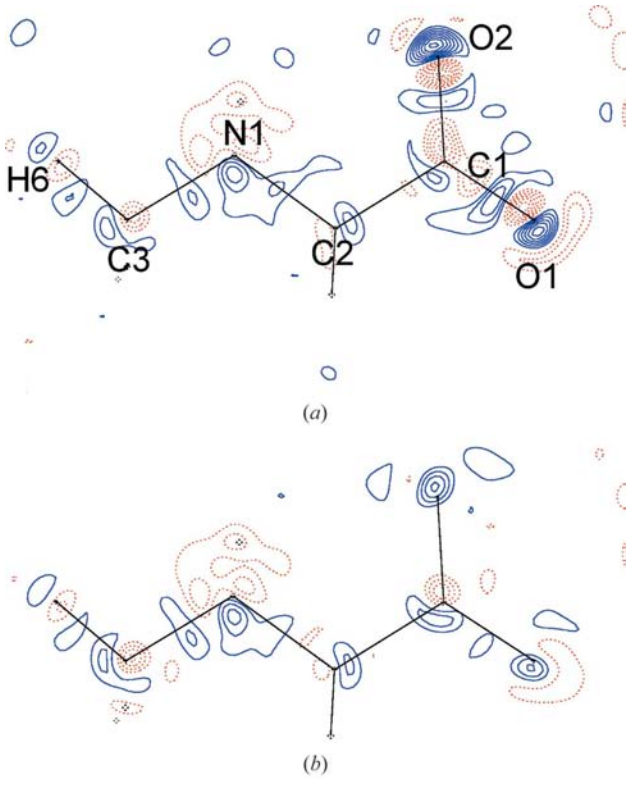

Figure 4
By including the κ' parameter (*b*) in the multipole model, unmodeled features in the Fourier residual electron density map (*a*) near the O-atom cores are reduced. Contour lines are 0.05 e Å^{-3} with blue indicating positive and red negative features.

6.5. Theoretical interaction density from the multipole model

To allow a comparison between theoretical and experimental results, we now try to obtain the interaction density using the density description of the multipole model. We

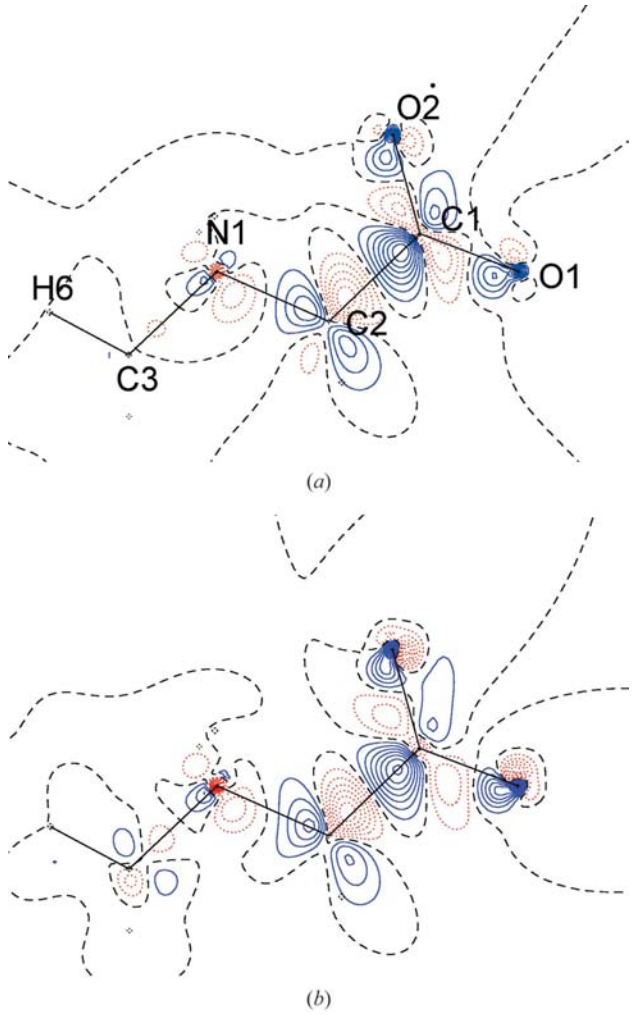

Figure 5
Interaction density as calculated from a difference of simulated structure factors from *CRYSTAL98* (Saunders *et al.*, 1998) (*a*) with κ parameters only and (*b*) including κ'. The same scales for contour lines as in Fig. 3(*b*) apply.

calculated the difference between the *CRYSTAL98* electron density and the *MOLSPLIT* isolated molecular density, both projected onto the multipole model that was also used in the experimental refinement *via* simulated structure factors. As stated before, unit weights were used in the refinement against simulated structure factors. Fig. 5 shows that, when the multipole model is used to represent the molecular electron density with simulated data to the resolution reached in the experiment, most features of the interaction density can be obtained. Fig. 5(*a*) was calculated using κ parameters only, whereas Fig. 5(*b*) included κ', and the two results agree qualitatively. Notably, use of a single κ' parameter for all higher multipoles leads to dramatically different (up to $\approx$0.2 e per atom) monopole populations. Both Figs. 5(*a*) and 5(*b*) can in principle be directly compared with the purely theoretical interaction density (Fig. 3) and show, as expected, similar results near the O atoms, and the C1—C2 and the C2—N1 bonds. However, features in the interaction density are not as pronounced as obtained directly from the theoretical electron density (Fig. 3*b*) and their character, especially of sharp core-polarization features near the nuclei, is blurred. Information on such sharp features is supposedly not available from the thermally smeared experimental structure factors. Close to N1, further differences are seen; the large and strongly negative region near N1 and the N1—C2 bond are not well reproduced by the multipole model. We suppose that, like in the case of the O atoms, this is due to the radial expansion/contraction parameters κ that might not be able to simultaneously fit electron-density features close to the nuclei and in regions of covalent bonding further away from it. Another influencing factor could be that the calculated H-atom ADPs are overestimated. Nevertheless, the interaction density from the multipole model has the advantage that it provides a realistic perspective on what result can currently be expected using experimental data.

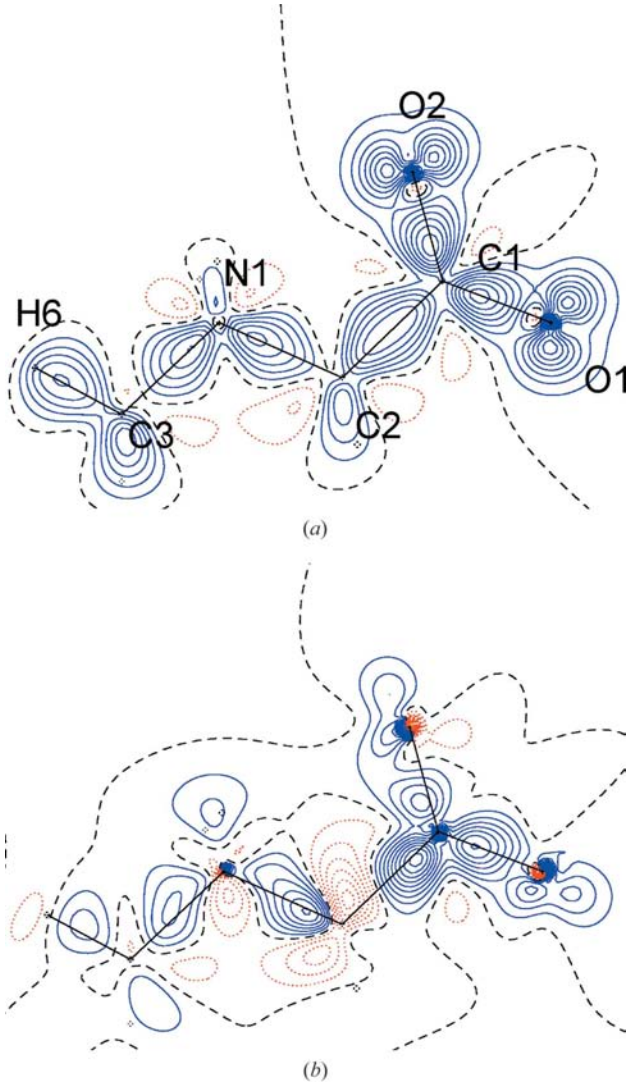

Figure 6
(*a*) Experimental deformation density obtained from *EXPER_MULT* and (*b*) *EXPER_MULT* − *THEOR_MOLE* difference between experimentally refined and calculated whole-molecule densities indicating crystal-field effects in a qualitative way. The same scales for contour lines as in Figs. 3(*a*) and 3(*b*) apply.

In contrast to κ, κ' parameters cannot be obtained from experiment in a reliable manner, and to be consistent with earlier charge-density studies we have chosen not to use κ' parameters for subsequent difference densities. In our opinion, a κ-only multipole model is equally as valid as a κ' restricted multipole model (Volkov *et al.*, 2001), since it remains unclear which κ' values are the appropriate choice for a molecule in a crystal. Taking into account their poor convergence, we do not consider κ' to be robust parameters in the description of electron density.

6.6. Comparison of experimental and single-point electron densities

It was stated previously that 'the effects of intermolecular interactions will be measurable in careful experiments ...' (Spackman *et al.*, 1999). To assess whether or not the interaction density is indeed accessible from experimental data, we calculated the difference between the experimentally refined and the isolated molecular density from theory. As the interaction density requires a calculation to provide a reference for an isolated molecule, we cannot obtain an interaction density purely from experiment unless we have two hypothetical crystal structures containing the same molecule with and without a hydrogen-bonding environment. Hence a single-point energy calculation based on the experimental geometry provided the wavefunction for simulating structure factors as described above.

In this way, scattering factors for a whole molecule projected onto the multipole model were generated and the interaction density was obtained by subtracting the pseudo-atomic density from a fit to these simulated structure factors from the density obtained from the experimentally refined population parameters. It is depicted in Fig. 6 in the same plane as for the interaction density from the *CRYSTAL98* calculation (Fig. 3) and similar features can be seen near the O atoms, on the C1—C2 bond and near C2. We cannot expect a complete agreement with the theoretical result (Fig. 3). Apart

from experimental uncertainties, the choice of a different method and basis set will also give rise to differences in the Hartree–Fock result. There are additional features that are not observed in the theoretical maps. These are most prominent on the C—O bonds and near the O-atom core, showing additional diffuse electron density near the lone pairs. As shown before in §6.5, the multipole model does not adequately reproduce sharp density features near the O-atom cores. Although additional electron density in the carboxylate groups is often observed in experimental charge-density studies as shown in numerous topological analyses, these features are influenced by the limited flexibility of the multipole model (Volkov & Coppens, 2001), and should be interpreted with caution. Using a more sophisticated density description than the multipole model (Jayatilaka & Grimwood, 2001) seems appropriate and will be the subject of future research. We note that, in addition to including anisotropic thermal motion for H atoms from theory, imposing the electron density of the H atoms from the invariom database was necessary to obtain the interaction density experimentally. It appears that such a highly constrained multipole model[3] is necessary to observe these fine details with current data, as the scattering signal of the H atoms is unfortunately rather small when compared to C, N or O atoms.

6.7. Obtaining an approximate interaction density using the invariom database

A single-point electron density based on the geometry found in the crystal followed by simulating structure factors and performing a multipole refinement can be a time-consuming and even infeasible task for a larger molecule. We have therefore tried to approximate the isolated-molecular electron density that has been projected onto the multipole model by the pseudoatoms of the invariom database, the aim being the ability to also employ invarioms for calculation of the interaction density. In Fig. 7(*a*), we have visualized electron-density differences between the sum of invariom fragments and multipole-projected isolated molecular density. It exhibits the same features as discussed earlier for the theoretical interaction density. Compared to the 'whole-molecule' approach, this difference density has the advantage that it can be rapidly obtained from the pre-determined invariom database entries. It furthermore allows one to validate a structural model and points to unmodeled features like disorder for example. To judge how well the invariom density resembles the whole-molecular density, we have subtracted the two, as shown in the right part of Fig. 7.

Subtle differences remain and are due to differences in the bond distances of model compounds and the experimental result. For example, in the model compound for the carboxylate group, the two bond distances are virtually the same in the geometry optimization, whereas in the experiment one bond is shorter, leading to the extra density in the database interaction density on the O2—C1 bond that can be seen in Fig. 7(*b*). Overall, we think that the performance of the database in reproducing a molecular density is satisfactory although the agreement between the experimentally refined and the invariom density is of the order of magnitude of the interaction density. The good agreement between a whole molecular density and the sum of the database fragments of $\approx$0.1 e Å^{-3} indicates that the invariom density is well suited for use in standard structural data where the electron density cannot be refined, providing support for the invariom approach.

To confirm our finding that the interaction density can be obtained also for this non-centrosymmetric structure either by 'whole molecule' or approximately by invariom scattering factors, we have calculated two Fourier residual maps (Fig. 8)

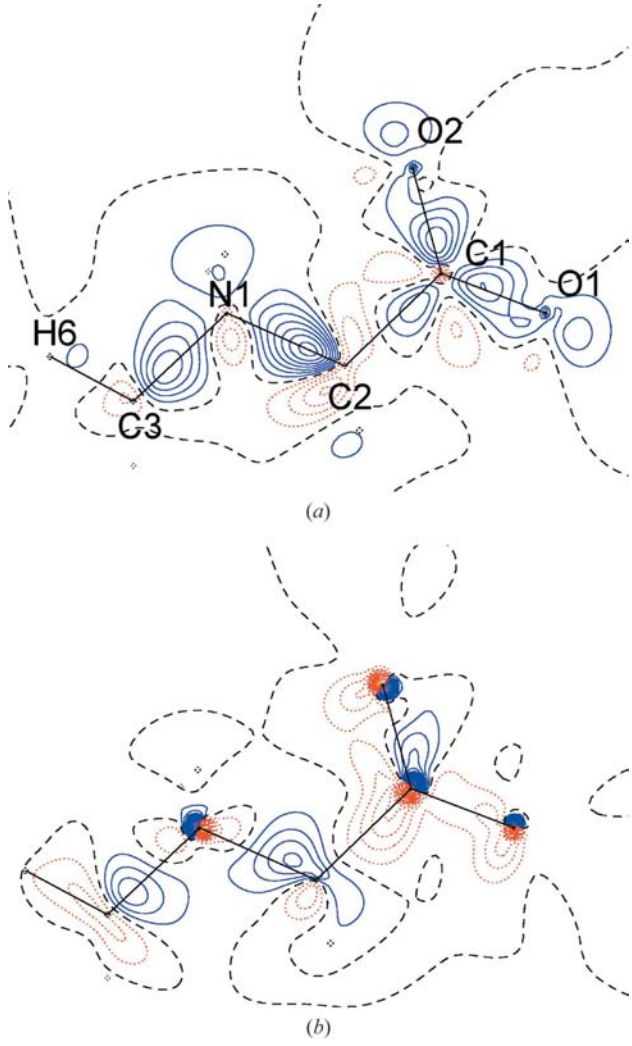

Figure 7
(*a*) Difference between experimentally refined and the density calculated from the invariom database parameters using the same geometry indicating crystal-field effects in a qualitative way. (*b*) Difference between the density from 'whole molecule' and invariom database parameters. Contour lines are 0.025 e Å^{-3} with blue indicating positive and red negative features.

[3] The procedure in this paper has been chosen to avoid potential problems arising from inadequate modeling of the thermal motion of the H atoms. Employing only isotropic temperature parameters for H atoms leads to correlations with their monopole parameters. These in turn can influence the monopole parameters of the C, N and O atoms because of the overall charge constraint.

Table 3
Dipole moments for sarcosine.

Method	Dipole moment (D)			Total
	x	*y*	*z*	
Invariom (*EXPER_INVM*)	7.3 (7)	−4.2 (1)	10.4 (5)	13.4 (6)
Experimental (*EXPER_MULT*)	6.9 (2)	−3.6 (1)	10.0 (3)	12.7 (2)
Multipole projected (*THEOR_MULT*)				
B3LYP/D95++(3df,3pd)	6.0 (1)	−3.0 (1)	8.8 (1)	11.1 (1)
Directly from theory (*THEOR_MOLE*)				
B3LYP/D95++(3df,3pd)	7.1	−2.6	10.1	12.6
Multipole projected crystal (*THEOR_CRYS*)				
PHF/6-31G(d,p)	6.0 (2)	−2.9 (2)	9.0 (3)	11.2 (2)
Multipole projected pseudocrystal (*THEOR_SPLT*)	5.7 (2)	−3.0 (2)	8.6 (3)	10.7 (2)

for the *EXPER_MULT* and the *EXPER_INVM* refinement. Whereas the experimental Fourier map is almost featureless and the remaining density is randomly distributed apart from remaining unfitted electron density near the back of the O atoms, the invariom map shows features similar to those seen in the theoretical (Figs. 3*b*, 5*a* and 5*b*) or the 'experimental' interaction densities (Figs. 6*b* and 7*a*). We suggest that as part of the procedure it should be verified if difference density features are supported by analogous features in the residual density maps.

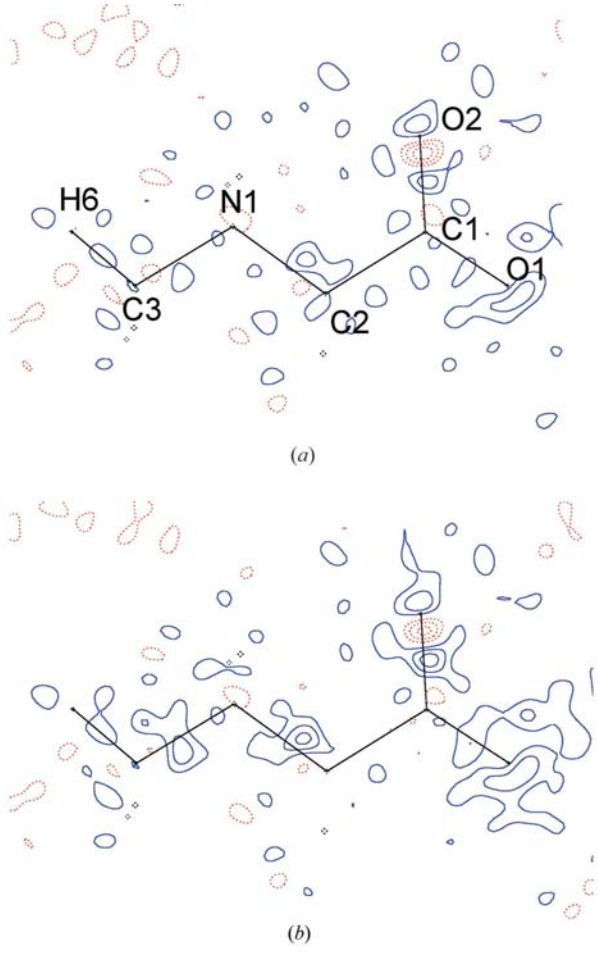

Figure 8
Fourier residual density maps for (*a*) the *EXPER_MULT* and (*b*) the *EXPER_INVM* refinement. Contour lines are 0.05 e Å^{-3} with blue indicating positive and red negative features. Unmodeled features in the invariom residual density resemble the interaction density.

6.8. Dipole moments

The dipole moment derived from a multipole model is a quantity very sensitive to even small changes in the monopole charges, which themselves, if experimentally determined, are affected by systematic errors in X-ray data sets. Quantitatively, the crystal-field effect often manifests itself in an increase of the dipole moment (Spackman *et al.*, 2007). As the sarcosine molecule is a zwitterion, a strong increase in the dipole moment is neither expected nor observed. Table 3 lists values of this quantity obtained from different electron densities using the same geometry. It can be seen that the dipole moment from experiment (*EXPER_MULT*) agrees well with the theoretical one as calculated directly from the D95++(3df,3pd) wavefunction (*THEOR_MOLE*), also taking into account the error range. Invariom refinement (*EXPER_INVM*) reproduces magnitude, direction and components of the theoretical dipole moment. Although database entries do not take into account polarization of the crystal field, the dipole moment is slightly higher than from theory or experiment. However, the invariom result has a higher error assigned to it, as it includes the standard uncertainties of a larger number of parameters. Within this error range, it agrees well with the other results. Multipole projection with simulated data (*THEOR_MULT*) reproduces the *ab initio* dipole moment only satisfactorily. The result of the multipole projection for the crystal (*THEOR_CRYS*) using the 6-31G(d,p) basis set is very close to this result; compared to the projection using the *MOLSPLIT* structure factors (*THEOR_SPLT*), a small dipole moment enhancement in the crystal within the error range can be observed.

7. Conclusions

In this work, we examine the interaction density of the non-standard amino acid sarcosine. A focus of this study is to show that the interaction density can be obtained from experiment. Based on purely theoretical methodology, the interaction density of sarcosine was found to be small (≤25%) compared to density accumulations in covalent bonds or lone pairs, but systematic. Earlier findings that the electron-density re-

arrangement due to hydrogen bonding in the crystal accounts for the crystal-field effect are supported.

The interaction density was also obtained as the difference between experimental charge density and theoretically derived isolated molecular density projected onto the multipole model. As only the density in the bulk can be determined by experiment, the experimental procedure requires a calculation of an isolated-molecular density or alternatively theoretically derived database parameters. An interesting aspect of studying fine features of the electron-density distribution in the crystal environment with the multipole model is that the interaction density maps agree only qualitatively with the periodic Hartree–Fock result. Limitations in the density description of the multipole model are becoming obvious and especially sharp features are not adequately described. On one hand, such features probably depend on how much information is available for high-angle data, which would make ever higher scattering angles a worthwhile aim in future studies; ultra-low temperatures would also be beneficial to the analysis. Such experiments require synchrotron radiation and are indeed possible for compounds like sarcosine. On the other hand, it remains an open question whether the use of the multipole model makes the analysis unnecessarily difficult or whether other, more modern, approaches like 'wavefunction fitting' might allow a more consistent answer.

To obtain the results, it is essential that the same geometry is used for experimental and theoretical densities. We carefully conclude that an approximate interaction density is accessible by experiment from a highly restricted multipole refinement. The interaction density is not yet well understood and further studies would be desirable.

Invariom modeling was used successfully to reproduce the theoretically derived isolated molecular density. Therefore, it can be used in place of a theoretical density projected onto the multipole formalism to calculate the interaction density. Using the invariom database, such an approximate interaction density can be observed by experiment also for larger molecules where crystal and data quality as well as the resolution are high. As the interaction density has a small overall effect on the electron density, the invariom approach is well suited to reproduce *dominant* features of the aspherical electron density in X-ray diffraction of organic molecules.

This work was supported by the Australian Synchrotron Research Program (ASRP), which is funded by the Commonwealth of Australia under the Major National Research Facilities Program. BD thanks the ASRP for a postdoctoral fellowship. We thank D. Jayatilaka for helpful discussions and improvements in the manuscript and T. Koritsánszky for source code of the locally modified version of *XDLSM* used.

References

Allred, A. L. & Rochow, E. G. (1958). *J. Inorg. Nucl. Chem.* **5**, 264–268.
Besler, B. H., Merz, K. M. & Kollman, P. A. (1990). *J. Comput. Chem.* **11**, 431–439.
Burnett, M. N. & Johnson, C. K. (1996). *ORTEP-III, Oak Ridge Thermal Ellipsoid Plot Program for Crystal Structure Illustrations.* Oak Ridge National Laboratory Report ORNL-6895, Oak Ridge, Tennessee, USA.
Bytheway, I., Chandler, G. S., Figgs, B. N. & Jayatilaka, D. (2007). *Acta Cryst.* A**63**, 135–145.
Clark, R. C. & Reid, J. S. (1995). *Acta Cryst.* A**51**, 887–897.
Clementi, E. & Raimondi, D. L. (1963). *J. Chem. Phys.* **38**, 2686–2689.
Clementi, E. & Roetti, C. (1974). *At. Data Nucl. Data Tables*, **14**, 177–478.
Coppens, P. (1997). *X-ray Charge Densities and Chemical Bonding. IUCr Texts on Crystallography*, No. 4. Oxford University Press.
Dapprich, S., Komáromi, I., Byun, K. S., Morokuma, K. & Frisch, M. J. (1999). *J. Mol. Struct. (Theochem.)*, **461**, 1–21.
Dittrich, B. (2007). *TLS+O, A Program to Prepare Input Files for QM/MM Cluster Calculations Using the TLS + ONIOM Approach.* University of Western Australia, Crawley, WA, Australia.
Dittrich, B., Koritsánszky, T. & Luger, P. (2004). *Angew. Chem. Int. Ed. Engl.* **43**, 2718–2721.
Dittrich, B., Whitten, A. & Spackman, M. (2005). *Acta Cryst.* A**61**, C420.
Gatti, C., Saunders, V. R. & Roetti, C. (1994). *J. Chem. Phys.* **101**, 10686–10696.
Gatti, C., Silvi, B. & Colonna, F. (1995). *Chem. Phys. Lett.* **247**, 135–141.
Gaussian 98 (2002). Revision A.11.3, by M. J. Frisch *et al.* Gaussian, Inc., Pittsburgh, PA, USA.
Hansen, N. K. & Coppens, P. (1978). *Acta Cryst.* A**34**, 909–921.
Hehre, W. J., Ditchfield, R., Stewart, R. F. & Pople, J. A. (1970). *J. Chem. Phys.* **52**, 2769–2773.
Hehre, W. J., Stewart, R. F. & Pople, J. A. (1969). *J. Chem. Phys.* **51**, 2657–2664.
Hirshfeld, F. L. (1976). *Acta Cryst.* A**32**, 239–244.
Hübschle, C. B., Luger, P. & Dittrich, B. (2007). *J. Appl. Cryst.* **40**, 623–627.
Jayatilaka, D. (1994). *Chem. Phys. Lett.* **230**, 228–230.
Jayatilaka, D. & Grimwood, D. J. (2001). *Acta Cryst.* A**57**, 76–86.
Jayatilaka, D. & Grimwood, D. J. (2003). *Computational Science – ICCS 2003*, **2660**, 142–151.
Keller, E. & Pierrard, J.-S. (1999). *SCHAKAL99.* University of Freiburg, Germany.
Koritsánszky, T., Richter, T., Macchi, P., Volkov, A., Gatti, C., Howard, S., Mallinson, P. R., Farrugia, L., Su, Z. W. & Hansen, N. K. (2003). *XD – a Computer Program Package for Multipole Refinement and Topological Analysis of Electron Densities from Diffraction Data.* Freie Universität Berlin, Berlin, Germany.
Koritsanszky, T., Volkov, A. & Coppens, P. (2002). *Acta Cryst.* A**58**, 464–472.
Kurki-Suonio, K. (1977). *Isr. J. Chem.* **16**, 115–123.
Madsen, A. Ø. (2006). *J. Appl. Cryst.* **39**, 757–758.
Madsen, A. Ø., Sørensen, H. O., Flensburg, C., Stewart, R. F. & Larsen, S. (2004). *Acta Cryst.* A**60**, 550–561.
Mostad, A. & Natarajan, S. (1989). *Acta Chem. Scand.* **43**, 1004–1006.
Oxford Diffraction Ltd (2006). *CrysAlis CCD and RED*, Version 1.171.31.5. Oxford Diffraction Ltd, Oxford, UK.
Platts, J. A. & Howard, S. T. (1996). *J. Chem. Phys.* **105**, 4668–4674.
Rappé, A. K., Casewit, C. J., Colwell, K. S., Goddard, W. A., Skid, W. M. & Bernstein, E. R. (1992). *J. Am. Chem. Soc.* **114**, 10024–10039.
Roversi, P. & Destro, R. (2004). *Chem. Phys. Lett.* **386**, 472–478.
Saunders, V. R., Dovesi, R., Roetti, C., Causà, M., Harrison, N. M., Orlando, R. & Zicovich-Wilson, C. (1998). *CRYSTAL98 User's Manual.* Universita di Torino, Torino, Italy.
Schomaker, V. & Trueblood, K. N. (1968). *Acta Cryst.* B**24**, 63–76.
Schomaker, V. & Trueblood, K. N. (1998). *Acta Cryst.* B**54**, 507–514.

Sheldrick, G. M. (1997). *SHELXL-97. A Program for Refinement of Crystal Structures.* University of Göttingen, Germany.
Spackman, M. A. & Byrom, P. G. (1996). *Acta Cryst.* B**52**, 1023–1035.
Spackman, M. A., Byrom, P. G., Alfredsson, M. & Hermansson, K. (1999). *Acta Cryst.* A**55**, 30–47.
Spackman, M. A., Munshi, P. & Dittrich, B. (2007). *Chem. Phys. Chem.* **11**, doi: 10.1002/cphc.200700339.
Stewart, R. F. (1976). *Acta Cryst.* A**32**, 565–574.
Volkov, A., Abramov, Y. & Coppens, P. (2001). *Acta Cryst.* A**57**, 272–282.
Volkov, A. & Coppens, P. (2001). *Acta Cryst.* A**57**, 395–405.
Vries, R. Y. de, Feil, D. & Tsirelson, V. G. (2000). *Acta Cryst.* B**56**, 118–123.
Whitten, A. E. & Spackman, M. A. (2006). *Acta Cryst.* B**62**, 875–888.